

University of Nebraska - Lincoln

DigitalCommons@University of Nebraska - Lincoln

Timothy J. Gay Publications

Research Papers in Physics and Astronomy

1992

An attempt to observe Mott scattering optically

J. E. Furst

University of Missouri - Rolla

Timothy J. Gay

University of Nebraska - Lincoln, tgay1@unl.edu

W. M. K. P. Wijayaratna

University of Missouri - Rolla

K. Bartschat

Drake University

H. Geesmann

Drake University

See next page for additional authors

Follow this and additional works at: <https://digitalcommons.unl.edu/physicsgay>



Part of the [Physics Commons](#)

Furst, J. E.; Gay, Timothy J.; Wijayaratna, W. M. K. P.; Bartschat, K.; Geesmann, H.; Khakoo, M. A.; and Madison, D. H., "An attempt to observe Mott scattering optically" (1992). *Timothy J. Gay Publications*. 58. <https://digitalcommons.unl.edu/physicsgay/58>

This Article is brought to you for free and open access by the Research Papers in Physics and Astronomy at DigitalCommons@University of Nebraska - Lincoln. It has been accepted for inclusion in Timothy J. Gay Publications by an authorized administrator of DigitalCommons@University of Nebraska - Lincoln.

Authors

J. E. Furst, Timothy J. Gay, W. M. K. P. Wijayaratna, K. Bartschat, H. Geesmann, M. A. Khakoo, and D. H. Madison

An attempt to observe Mott scattering optically

J E Furst†, T J Gay†, W M K P Wijayarathna†, K Bartschat‡,
H Geesmann†§, M A Khakoo†|| and D H Madison†

† Physics Department and Laboratory of Atomic and Molecular Research, University of Missouri-Rolla, Rolla, MO 65401, USA

‡ Physics and Astronomy Department, Drake University, Des Moines, IA 50311, USA

Received 11 September 1991

Abstract. We report an attempt to make an optical observation of Mott scattering, involving the first studies of inelastic collisions between polarized electrons and a heavy noble gas. Polarization fractions of light emitted by the $5p^56p[{}^3_2]_3({}^3D_3)$ state of Xe following impact excitation in an axial collision geometry were measured as a function of the incident electron energy, and compared with distorted-wave Born calculations. The theoretical and experimental results agree qualitatively in the energy range where cascade contributions to the photon signal are small. We failed to measure non-zero values of the linear polarization fraction η_1 , which would have constituted unambiguous evidence for Mott scattering and/or the importance of higher-order excitation processes in this system.

1. Introduction

When atomic targets are excited by fast projectiles, the radiation emitted by the excited atoms is generally polarized. Measurement of the polarization is a good way to study the excitation dynamics (Andersen *et al* 1988, Blum 1981, Fano and Macek 1973). The types of polarization that do not vanish in a given collision depend on its symmetry; a number of possible symmetries are illustrated in figure 1. Consider the simplest possible axial collision geometry (figure 1(a)). If the initial momenta of the (unpolarized) projectiles define the \hat{z} axis and photons are observed along \hat{y} , then for an isotropic target and no detection of the scattered projectiles the only standard component of polarization which can be non-zero is

$$\eta_3 \equiv \frac{I(0^\circ) - I(90^\circ)}{I(0^\circ) + I(90^\circ)} \quad (1)$$

where $I(\theta)$ is the intensity of light polarized along the axis which makes an angle θ with \hat{z} (figure 1). If the collision symmetry is reduced so that an axial vector is now geometrically defined along \hat{y} , then two more polarization fractions may be non-zero:

$$\eta_1 \equiv \frac{I(45^\circ) - I(135^\circ)}{I(45^\circ) + I(135^\circ)} \quad (2)$$

and

$$\eta_2 \equiv \frac{I(\sigma^+) - I(\sigma^-)}{I(\sigma^+) + I(\sigma^-)} \quad (3)$$

§ Present address: Physikalisches Institut, Universität Münster, Federal Republic of Germany.

|| Permanent address: Physics Department, California State University-Fullerton, Fullerton, CA 92634-9480, USA.

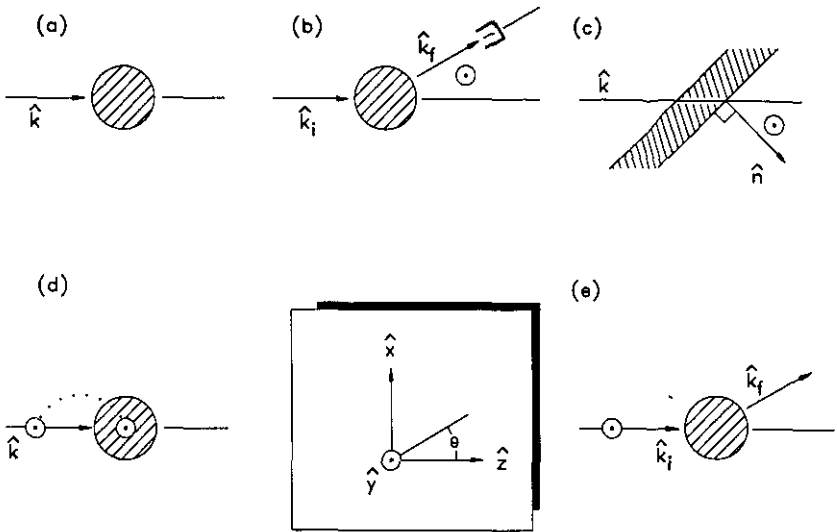


Figure 1. Various collision symmetries. Axial vectors defined by the collision geometry ((b) and (c)) or the electron polarization ((d) and (e)) are indicated by concentric circles and dots. The coordinate system for the discussion in the text and this figure is shown between (d) and (e).

where σ^+ (σ^-) corresponds to right-(left-)handed circularly polarized light. Such symmetry breaking occurs, for example, if the photons are observed in coincidence with deflected projectiles (figure 1(b)) or if, in the case of beam-foil excitation, the foil normal is tilted away from \hat{z} (figure 1(c)).

Another way to introduce an axial vector into the collision geometry is to use transversely spin-polarized electrons as the incident particles, while retaining the azimuthal symmetry of the target and projectile-detection geometries. If a target electron is replaced by one from the polarized incident beam in an exchange excitation, the atom may become spin-oriented ($\langle S_y \rangle \neq 0$). When subsequent optical transitions are observed between states $|i\rangle$ and $|f\rangle$ with well defined total electronic angular momenta J_i and J_f , this spin orientation leads to non-vanishing values of η_2 . The first successful optical electron polarimeter was based on this principle (Farago and Wykes 1969, Wykes 1971, Eminyañ and Lampel 1980; see also, e.g., Naß *et al* 1988). Even if the fine-structure of the excited state is unresolved, residual spin-orbit coupling in the atom can, after some time interval, convert spin orientation to orbital orientation for excited states with $L > 0$, resulting in circular polarization of the emitted light (Gay 1983, Goeke *et al* 1987). These considerations apply as well to the case of direct excitation when the initial target state is electron-spin polarized (Jitschin *et al* 1984).

Non-zero values of η_2 may also result from asymmetric deflection of the polarized incident electrons caused by spin-orbit forces, or Mott scattering (figure 1(e)). In this case, a net orbital orientation of the target ($\langle L_y \rangle \neq 0$) can be produced directly during the collision. Mott scattering can be expected to cause appreciable values of η_2 only for high- Z atoms.

The linear polarization fraction η_1 may or may not vanish, depending on the angular momentum coupling of the excited state and the excitation dynamics. Bartschat and Blum (1982; see also Bartschat *et al* 1982, Bartschat 1989) have considered scattering-angle-integrated experiments involving collisions in which the total (target plus

continuum electron) spin and orbital angular momenta can be decoupled, i.e. described in an LS coupling scheme. They found that

$$\eta_1 = C \sum_K \left[(2K+1)^{1/2} (2J+1) (KQkq|21) \begin{Bmatrix} K & k & 2 \\ L & S & J \\ L & S & J \end{Bmatrix} A_{KQ}(L) O_{kq}(S) \right] \quad (4)$$

$$k = q = 1 \quad K = 2, 0 \quad Q = 0$$

where L , S , and J refer to the excited atomic state, A is the atomic orbital alignment tensor, O is the spin orientation tensor and C is a numerical constant. The two symbols in parentheses and brackets preceding A_{KQ} are Clebsch-Gordan and $9-j$ coefficients, respectively.

When the atomic excited states are well LS coupled, this expression for η_1 is identically zero. It is instructive to consider processes which invalidate equation (4):

(i) Exchange excitation of states which are not well LS coupled (figure 1(d)). For such states (e.g., the 6^3P_1 states of Xe and Hg) the L and S appearing in the $9-j$ symbol are not generally good quantum numbers. As a result, the symmetry properties of the $9-j$ no longer require η_1 to vanish. Moreover, the restrictions on K , Q , k and q are lifted because the alignment and orientation tensor components of the excited state can no longer be factored into time-independent L and S terms. This coupling of L and S , or equivalently, orientation and alignment, results from the strong magnetic forces in the atom responsible for the breakdown of the LS coupling scheme. Electron exchange is still required for η_1 to be non-zero.

(ii) Mott scattering (figure 1(e)). Even if the final state is well LS coupled, an asymmetric scattering process eliminates the restrictions on K and Q , i.e. alignment tensor components other than that corresponding to the second moment of electron distribution along \hat{z} can be non-zero. Specifically, η_1 can be non-zero with or without electron exchange when $K=2$ and $Q=1$. Again, Mott scattering will be important only with high- Z targets.

(iii) Higher-order scattering processes (figure 1(e)). It is possible, in principle, for excitation to occur in which the final state is well LS coupled but which proceeds during the collision time by temporary population of a non- LS coupled intermediate state (or states). In other words, spin-orbit forces could decouple L and S for the target electrons during the collision, even though the asymptotic state is well LS coupled. Such processes would allow $\eta_1 \neq 0$ by a lifting of the restriction on K , Q , k and q during the collision time with a subsequent 'freezing-in' of, e.g., $K=2$ and $Q=1$ in the final state. This could occur with or without electron exchange. The consequences of higher-order processes are essentially indistinguishable from those of Mott scattering.

The polarization of light emitted in scattering-angle-integrated experiments will generally depend on a combination of the mechanisms listed above. It is useful to try to disentangle their effects, and to assess their relative importance. Often, theoretical analyses of atomic scattering assume the validity of LS coupling during the collision and/or a lack of spin-orbit forces on the continuum electron. Perturbative methods have almost invariably ignored higher-order processes with heavy targets. Observations of polarization effects due to specific mechanisms can thus provide rigorous tests of such assumptions.

In the experiment reported here, we have attempted to make an unequivocal optical observation of Mott scattering (possibly in combination with higher-order effects) by studying excitation of an LS coupled state in a heavy atom. The polarization effects

of Mott scattering have probably been observed in several previous experiments with heavy targets, but they were not clear-cut. Non-zero values of η_2 are ambiguous because they can be caused by simple exchange excitation. In experiments by the Münster group (Bartschat *et al* 1982, Wolcke *et al* 1983), non-zero η_1 values were reported for Hg, where Mott scattering is certainly important. They considered, however, excitation of the 6^3P_1 level, which is not well *LS* coupled. Thus, again, the evidence for Mott scattering was obscured by other dynamical effects.

The experiment of Jitschin *et al* (1984) might have produced such evidence, in that they considered excitation of well *LS* coupled states, but their target was Na, in which spin-orbit forces on the continuum electron should be very small (see, e.g., McClelland *et al* 1990). More recently, Eschen *et al* (1989), in an experiment similar to that of Jitschin *et al*, used a Cs target, for which Mott scattering could possibly be expected to produce non-zero η_1 values (Nagy *et al* 1984). Unfortunately, neither group was specifically interested in isolating the effects of continuum spin-orbit forces as such, and their reported measurements of η_1 are cursory. Jitschin *et al* observed that '[η_1] was found to vanish within the experimental uncertainty [of 0.015],' and Eschen *et al* found η_1 to have 'small values' (which, from figure 9 of their report, appear to be consistent with zero).

We used a Xe target, which has a *Z* comparable to that of Cs. Moreover, Xe exhibits generally larger elastic Mott asymmetries than does Cs at low energies (Klewer *et al* 1979a, b), which suggests that a non-zero η_1 might be observable with this target. In addition to careful measurements of η_1 , we have determined η_2 and η_3 as a function of incident electron energy. This is the first experimental study of inelastic collisions between polarized electrons and a heavy noble gas. The $5p^56p[\frac{5}{2}]_3(^3D_3)$ state of Xe (Moore 1971) is the only one which has the combination of good *LS* coupling, an optical decay path ($6^3D_3-5p^56s[\frac{3}{2}]_3(^3P_2)$; 882 nm), and adequate separation in energy from the next higher intermediately-coupled state which could populate it by cascade decay. The latter criterion is important because it is desirable to make measurements at energies well above the excitation threshold of the primary state, to minimize statistical uncertainty, while cascade contributions from higher-lying non-*LS* coupled states compromise the measurement. Since our electron beam has an energy width of ~ 0.2 eV, it is straightforward to separate the 6^3D_3 state, with a threshold at 9.72 eV, from the nearest non-*LS* coupled state ($5p^55d[\frac{7}{2}]_3(^3F_3)$) with a threshold at 10.04 eV. A concomitant advantage of the 6^3D_3 state is that radiation trapping, a potentially serious problem with the $^2P_{3/2,1/2}$ states studied in the alkalis, is negligible.

2. Experiment

The experimental apparatus is shown schematically in figure 2 (Gay *et al* 1992). Longitudinally polarized electrons are produced by photoemission from a GaAs crystal. The beam of electrons extracted from the crystal is bent by 90° in a spherical electrostatic deflector and thus becomes transversely polarized. Upon exiting the source chamber, the beam enters a concentric-cylinder Mott analyser where its degree of polarization can be determined, and then passes through a solenoidal spin rotator before entering the target chamber.

In the target chamber, the beam is decelerated to the requisite collision energy before colliding with an effusive beam of Xe directed downward into a 2300 l s^{-1} diffusion pump. Light emitted from the collision volume towards the optical polarimeter

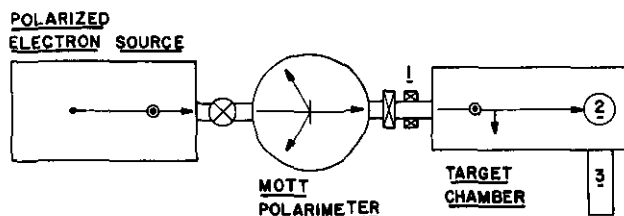


Figure 2. Schematic diagram of the experimental apparatus showing, in particular, the spin rotator (1), Xe target (2), and optical polarimeter (3).

is collected and focused to a parallel beam by a spherical lens which is an integral part of the target-chamber vacuum wall. The light then passes through a polarizing film, a quarter-wave retarder, and a narrow-band interference filter before being refocused onto the GaAs photocathode of a cooled photon-counting photomultiplier tube. For measurements of η_1 and η_3 , the polarizer and retarder are rotated together to minimize the optical train's instrumental polarization. For η_2 measurements, the linear polarizer and retarder positions are switched, and only the retarder is rotated. In the case of η_1 and η_2 , which are proportional to the electron beam polarization, P , instrumental asymmetries can be eliminated by flipping the incident electron polarization optically in the GaAs source.

The absolute energy scale for our measurements was set by determining the voltage corresponding to the onset of photon production from the target, and setting it equal to 9.72 eV, the 6^3D_3 threshold. Because the excitation onset is associated with the highest energy electrons in the beam (at the top of a ~ 0.2 eV wide distribution), cascading from higher-lying states is eliminated by remaining at or below 10.0 eV on this scale. Background subtraction can be a serious problem near threshold where count rates are relatively low. Background sources in this experiment were photomultiplier tube dark count, a weakly energy-dependent electron-beam-related signal with no target gas, and a small residual contribution from electron-gas collisions occurring outside the direct line-of-view of the optical train.

Measurements of η_1 and η_2 made with two electron helicities indicated that instrumental asymmetries in the optical train were ≤ 0.01 for both circular and linear polarization analysis. These asymmetries could be eliminated in the η_1 and η_2 results, but we expect our η_3 measurements, which are spin-independent, to be systematically in error by an amount of the order of ± 0.01 .

3. Results

Results for η_2 and η_3 between 9.5 and 100 eV are shown in figures 3–6. Shown also are the results of new first-order distorted-wave Born approximation (DWBA) calculations which include spin-orbit forces on the continuum electron, and which provide a theoretical benchmark for our measurements (Barschat and Madison 1987).

At threshold the values of η_2 and η_3 are constrained kinematically, because the 3D_3 state must be excited solely by exchange (which is true at all energies), and only the states with initial values of $L_z = 0$ may be populated. Taking into account isotopic abundances and hyperfine depolarization effects, these values are $\eta_2 = 0.708P$, and $\eta_3 = 0.387$ (see, e.g., Wolcke *et al* 1983). Given a typical electron beam polarization

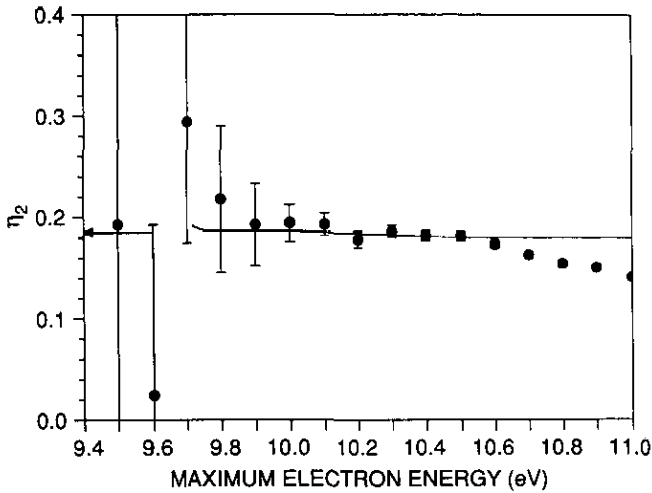


Figure 3. Circular polarization fraction η_2 for the 882 nm, $5p^56p(^3D_3) \rightarrow 5p^56s(^3P_2)$ transition in Xe as a function of maximum energy of the bombarding electron beam. The arrow indicates the kinematically determined threshold value for η_2 of 0.184 for an electron polarization $P=0.26$. The threshold energy is 9.72 eV. Experimental uncertainties are statistical only; DWBA theory is shown by the solid line connecting discrete calculated points.

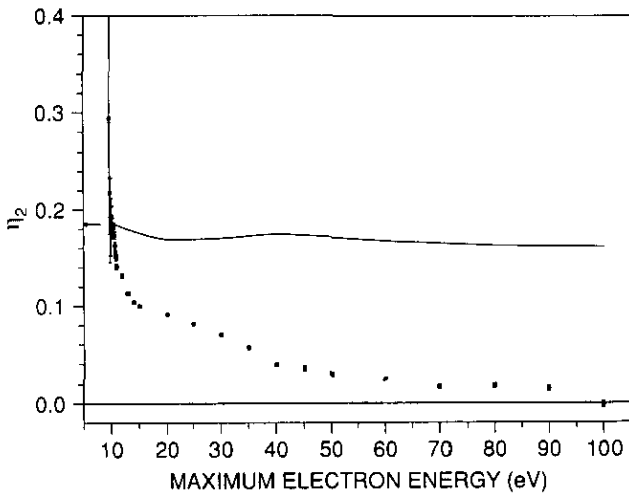


Figure 4. Data as in figure 3 over a larger energy range.

of 0.26, both experimental threshold limits are consistent with these kinematic values. Moreover, the polarization fractions make a discontinuous transition from their threshold values to values consistent with zero at an energy of 9.6 eV, independently defined using a separate excitation run. This gives us confidence that our background subtraction procedure near threshold is proper.

As the beam energy is increased above 10 eV, cascading begins to affect the polarization. In the high energy limit, the ratio of exchange to direct excitation cross sections vanishes, so all the photons detected will have resulted from cascades from non- LS coupled states with singlet components. Thus η_2 must approach zero, since

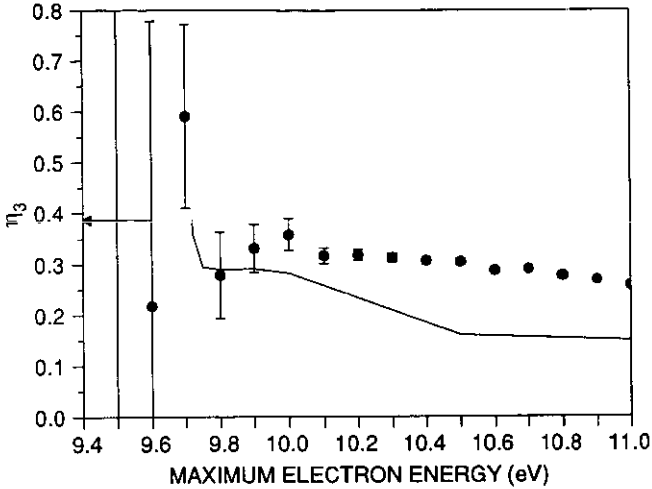


Figure 5. The linear polarization fraction η_3 versus maximum electron energy. Kinematic threshold limit of 0.387 indicated.

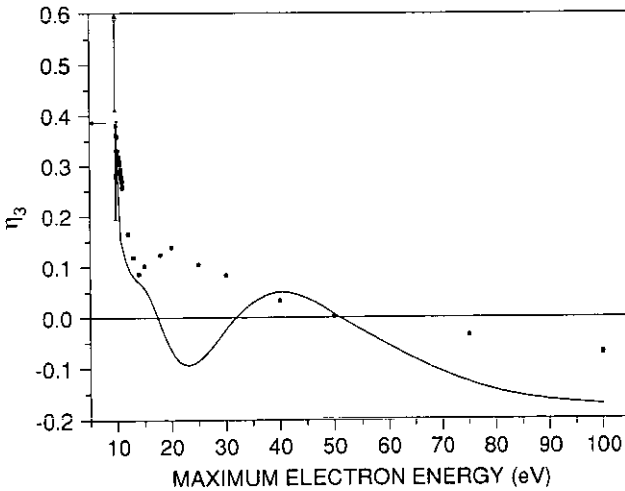


Figure 6. Data as in figure 5 over a larger energy range.

no spin polarization is transferred to the atom in a direct process. In addition, only $|L_z| = L$ states are excited in the high-energy limit, because longitudinal momentum transfer from the fast electron vanishes (Fano and Macek, 1973). This forces η_3 to be negative no matter which states are initially populated. The importance of cascading invalidates any comparison between experiment and theory above 10 eV; below 10 eV the agreement between the two is good (figures 3, 5), although one must remember that they are constrained to have the same value at 9.7 eV.

Finally, we have measured η_1 at 9.9 eV to be 0.004 ± 0.006 . This statistical accuracy required approximately 50 h of running time, exclusive of periodic excitation function checks of the beam energy. Our subsequent theoretical calculation of η_1 at this energy is -2.6×10^{-5} , assuming $P = 0.26$. It appears that, at least with Xe, optical observations of Mott scattering are not immediately feasible. Thus, integrated spin-orbit forces on

the continuum electron, possibly in combination with the effects of higher-order processes, are surprisingly small for this relatively high-Z target. Mercury targets might yield evidence for a Mott polarization effect. We suggest the $5d^{10}6s6d(^3D_3)-5d^{10}6s6p(^3P_2)$, 365 nm transition as a promising candidate for such an experiment.

Acknowledgment

This work was supported by National Science Foundation grants PHY-9007721, PHY-9014103, and PHY-8813799. We thank Gy Csanak for useful conversations.

References

- Andersen N, Gallagher J W and Hertel I V 1988 *Phys. Rep.* **165** 1
 Bartschat K 1989 *J. Phys. B: At. Mol. Opt. Phys.* **22** 2917
 Bartschat K and Blum K 1982 *Z. Phys. A* **304** 85
 Bartschat K and Madison D H 1987 *J. Phys. B: At. Mol. Phys.* **20** 5839
 Bartschat K, Hanne G F and Wolcke A 1982 *Z. Phys. A* **304** 89
 Blum K 1981 *Density Matrix Theory and Applications* (New York: Plenum)
 Eminyan M and Lampel G 1980 *Phys. Rev. Lett.* **45** 1171
 Eschen F, Hanne G F, Jost K and Kessler J 1989 *J. Phys. B: At. Mol. Phys.* **22** L455
 Fano U and Macek J 1973 *Rev. Mod. Phys.* **45** 553
 Farago P S and Wykes J S 1969 *J. Phys. B: At. Mol. Phys.* **2** 747
 Gay T J 1983 *J. Phys. B: At. Mol. Phys.* **16** L553
 Gay T J, Khakoo M A, Brand J A, Furst J E, Meyer W V, Wijayaratna W M K P and Dunning F B 1992 *Rev. Sci. Instrum.* in press
 Goetze J, Kessler J and Hanne G F 1987 *Phys. Rev. Lett.* **59** 1413
 Jitschin W, Osimitsch S, Reihl H, Kleinpoppen H and Lutz H O 1984 *J. Phys. B: At. Mol. Phys.* **17** 1899
 Klewer M, Beerlage M J M and van der Wiel M J 1979a *J. Phys. B: At. Mol. Phys.* **12** 3935
 — 1979b *J. Phys. B: At. Mol. Phys.* **12** L525
 McClelland J J, Buckman S J, Kelley M H and Celotta R J 1990 *J. Phys. B: At. Mol. Opt. Phys.* **23** L21 and references therein
 Moore C E 1971 *Atomic Energy Levels* vol 3, NSRDS-NBS 35 (Washington, DC: US Govt Printing Office)
 Nagy O, Bartschat K, Blum K, Burke P G and Scott N S 1984 *J. Phys. B: At. Mol. Phys.* **17** L527
 Naß P, Eller M, Ludwig N, Reichert E and Webersinke M 1989 *Z. Phys. D* **11** 71
 Wolcke A, Bartschat K, Blum K, Borgmann H, Hanne G F and Kessler J 1983 *J. Phys. B: At. Mol. Phys.* **16** 639
 Wykes J W 1971 *J. Phys. B: At. Mol. Phys.* **4** L91